Thermoelectric Properties of $Zr_3Mn_4Si_6$ and $TiMnSi_2$

Ryosuke O. Suzuki *,** and Hirotake Kozasa***

Department of Materials Science, Hokkaido University

N13W8 Kita-ku, Sapporo 060-8628, Hokkaido, Japan

Abstract

The Seebeck coefficient, electrical resistivity, and thermal conductivity of $Zr_3Mn_4Si_6$ and $TiMnSi_2$ were studied. The crystal lattices of these compounds contain relatively large open spaces, and therefore, they have fairly low thermal conductivities (8.26 and 6.63 $Wm^{-1}K^{-1}$, respectively) at room temperature. Their dimensionless figures of merit *ZT* were found to be 1.92×10^{-3} (at 1200 K) and 2.76×10^{-3} (at 900 K), respectively. The good electrical conductivities and low Seebeck coefficients may possibly be due to the fact that the distance between silicon atoms in these compounds is shorter than that in pure semiconductive silicon.

Keywords: thermal conductivity, silicide, Seebeck coefficient, electrical resistivity, layered structure

* Corresponding author: e-mail: rsuzuki@eng.hokudai.ac.jp

** CREST researcher, Japan Science and Technology Agency (JST)

*** Graduate Student, Hokkaido University

1. Introduction

Thermoelectronic materials are used in two applications: Peltier cooling and thermoelectric power generation. The Peltier effect is the generation of a temperature difference using electricity, whereas the Seebeck effect is the conversion of a temperature difference into electricity. The electricity generated in a thermoelectric material gradually decreases with the temperature difference, when heat flows from a thermal source at a higher temperature to a part at a lower temperature through thermoelectric materials. Therefore, thermoelectric materials with low thermal conductivity are required for power generation. The figure of merit Z has been used to evaluate this specific characteristic of thermoelectric materials.

$$Z = S^2/(\rho\,\kappa) \tag{1}$$

where S, ρ, and κ are the Seebeck coefficient, electrical resistivity, and thermal conductivity, respectively. Z is a valid parameter when the heat sources for the thermoelectric modules are kept at a constant temperature. However, one of the authors[1–4] noted that other factors such as fluid velocity can contribute to higher thermoelectric power generation when two thermal fluids are employed. In this case, it was also reported that materials with lower thermal conductivity are more favorable for maintaining a constant temperature difference, although it is necessary to evaluate these thermoelectric materials using Z. Recent studies have found many thermoelectric oxides having lower thermal conductivity that are suitable for power generation[5–8].

This study focuses on a new thermoelectric compound that contains metals that are abundant in nature. Iron alloys such as Fe_2VAl Heusler alloys[9,10] have been

reported previously; however, other metallic compounds have not been surveyed extensively. It is known that titanium (Ti) and zirconium (Zr) have lower thermal conductivity. Investigations of ternary intermetallic compounds containing Ti or Zr as the main component have revealed that a series of intermetallic compounds have interesting crystal structures that large vacant spaces are contained within their unit cells[11,12]. It was postulated that these compounds would have low thermal conductivity because the open spaces in their structures can lead to phonon scattering and energy loss.

Fig. 1 shows the crystal structure of $Zr_3Mn_4Si_6$ (tetragonal, D_{4h}^{13}-$P4_2/mbc$)[11] and $TiMnSi_2$ (orthorhombic, Pbam)[12]. $Zr_3Mn_4Si_6$ has a complex crystalline structure; for instance, Si-centered square antiprisms are unisotropically surrounded by Mn-centered octahedrals with a weak bond. The relatively wide open spaces and nonlinear atomic connections in a $Zr_3Mn_4Si_6$ crystal may cause stronger phonon scattering, which can lead to lower lattice conductivity, i.e., a more prominent thermal insulating property.

Tkachuk[11] reported that the crystal structure of $Zr_3Mn_4Si_6$ can be maintained when Zr is replaced by Hf. Unfortunately, a compound with the molecular formula $Ti_3Mn_4Si_6$ does not exist, although Ti, which belongs to the same group in the periodic table as Hf, is much cheaper and more abundant in nature than Hf. In the ternary system of Ti-Mn-Si, the existence of a compound, $TiMnSi_2$[12], having a composition similar to that of $Ti_3Mn_4Si_6$ was reported.

As shown in Fig. 1(c), $TiMnSi_2$ consists of Si layers that are packed between blocks of $Ti_2Mn_3Si_4$, so that it exhibits heat isolation such as that exhibited by the layered structure in Bi_2Te_3 or layered oxides.

2. Experimental

Mixtures of pure metals were melted in an argon-arc melting furnace to produce alloy ingots. The chemical composition of an ingot was analyzed at several points by a fluorescent X-ray analyzer (JOEL JSX-3220). As shown in Table 1, the analytical values were in good agreement with the stoichiometric ratio. Rectangular sections were cut from the ingots and used as samples for the analysis of thermoelectric properties.

The Seebeck coefficient of the sample (typical dimensions: 20 mm × 10 mm × 20 mm) was determined by inducing a temperature difference of 5–20 K in the sample by the natural temperature distribution in an electric furnace and then measuring the thermoelectromotive force[9]. The Seebeck coefficient was recorded continuously at temperatures ranging from room temperature to 1200 K. The electrical resistivity of another sample (dimensions: 2 mm × 8 mm × 12 mm) was measured by the standard four-probe method. The thermal conductivity and heat capacity of a cylindrical sample (diameter: 10 mm and thickness: 1.5 mm) were determined by the laser flash method (ULVAC TC-7000) for temperatures ranging from room temperature to 1100 K.

3. Results

3.1 Seebeck coefficient and electrical resistivity

Figs. 2 and 3 show the Seebeck coefficient S and the specific electrical resistivity ρ of $TiMnSi_2$ and $Zr_3Mn_4Si_6$. The Seebeck coefficients of both samples were positive, and they increased with temperature. The highest values of the Seebeck

coefficients of $TiMnSi_2$ and $Zr_3Mn_4Si_6$ were 27.0 μV/K at 1180 K and 28.8 μV/K at 1177 K, respectively. $Zr_3Mn_4Si_6$ exhibited metallic behavior: its electrical resistivity increased with temperature. However, the resistivity of $TiMnSi_2$ decreased as the temperature increased above 678 K, and it reached a minimum of 11.3 μΩm at 776 K. The electrical resistivity of $TiMnSi_2$ at room temperature was nearly equal to that of pure metals, which is a desirable characteristic for thermoelectric power generation.

Because the measured values of the Seebeck coefficient and electrical resistivity of $TiMnSi_2$ and $Zr_3Mn_4Si_6$ are as small as those of typical metals, our samples are analyzed using Mott's equation, which is often applied to the analysis of metals. The theoretical formula of the Seebeck coefficient according to Motts' theory[13] is given as

$$S = \frac{\pi^2}{3}\frac{{k_B}^2 T}{e}\left(\frac{1}{D(E)}\frac{\partial D(E))}{\partial E} + \frac{1}{F(E)}\frac{\partial F(E)}{\partial E}\right)_{E=\xi} \quad (2)$$

where e, k_B, T, E, $D(E)$, ξ, and $F(E)$ are the electric charge of carriers, Boltzmann constant, temperature, energy, density of state, chemical potential, product of the group velocity of carriers, and relaxation time, respectively. Here, $F(E)$ is assumed to be independent of energy.

According to this theoretical formula, the Seebeck coefficient is inversely proportional to the absolute value of $D(E)$ at the Fermi level (E_F) and directly proportional to the energy slope at E_F. Because $D(E)$ of the two intermetallic compounds have not been reported thus far, it is difficult to determine the state of the electric carriers around the Fermi surface. A continuous $D(E)$ and a free

electron approximation can, however, be assumed on the basis of the low electrical resistivity and the dependency of this electrical resistivity on temperature. Pseudogaps, which are generally observed in quasicrystals and Fe_2VAl[10], and a discontinuous $D(E)$ at E_F such as that for semiconducting Bi_2Te_3 and half-metals are not expected for these compounds. If Mott's theory is applied to the studied samples, the value of the Seebeck coefficient decreases as a result of a large number of carriers $N(E_F)$ and a small $\partial D(E)/\partial E$ because of a continuous $D(E)$ at E_F. On comparing these intermetallic compounds with typical metals in cases where Mott's theory is valid, it was observed that the Seebeck coefficient of pure iron is approximately 10 μV/K, and the Seebeck coefficients of Ti and Zr are 4.5 and 9.5 μV/K, respectively[14].

3.2 Thermal conductivity and ZT

Figs. 4–6 and Table 2 show the measured thermal diffusivity α and specific heat c_p of $Zr_3Mn_4Si_6$ and $TiMnSi_2$. The thermal conductivity κ was calculated as

$$\kappa = \alpha \cdot c_p \cdot d \tag{3}$$

The densities d of $TiMnSi_2$ and $Zr_3Mn_4Si_6$ were evaluated as 4.91 and 5.87 g/cm^3, respectively, using crystallographic data[11,12].

Z was evaluated using Eq. (1). As shown in Fig. 7, the dimensionless figures of merit ZT for $Zr_3Mn_4Si_6$ and $TiMnSi_2$ were estimated as 1.92×10^{-3} (1200 K) and 2.76×10^{-3} (900 K), respectively.

4. Discussion

Table 2 shows the specific heat and thermal conductivity of $Zr_3Mn_4Si_6$ and

$TiMnSi_2$ calculated by using the empirical Neumann-Kopp law in comparison with the measured values determined by the laser-flash method. There were slight differences between the values calculated using the Neumann-Kopp law and the measured values. The thermal conductivities of the two compounds were lower than those of typical metallic compounds[14]; this was in good agreement with the expected characteristics of the crystal structures. However, the Seebeck coefficients were very low for thermoelectric power generation, as shown in Fig. 2.

One of the reasons for the low values of the Seebeck coefficients may be the charge transfer of the excess carrier, which is attributed to the Si-Si bond in the crystal structure. A magnified view of a part of the crystal lattice of $Zr_3Mn_4Si_6$ is shown in Fig. 8. The Si-Si bonds, indicated by gray lines in figures (a, b, c-i, and c-ii), are 0.2346, 0.2553, 0.2766, and 0.2363 nm in length, respectively[11]. When silicon with a diamond structure has semiconducting properties, its Si-Si bond length is evaluated as 0.2822 nm[12]. Since the Si-Si bond length of $Zr_3Mn_4Si_6$ crystal is much shorter than that of silicon with a diamond structure, $Zr_3Mn_4Si_6$ has a more closely packed structure concerning the Si-Si distance. Therefore, electrons in the short Si-Si bond of $Zr_3Mn_4Si_6$ crystal may be easily transferred as in the case of a metallic bond. As a result, the values of both the Seebeck coefficient and the electrical resistivity of $Zr_3Mn_4Si_6$ are similar to those of a metallic structure.

Similarly, an Si-Si bond can be found in $TiMnSi_2$, as shown in Fig. 9. The length of this Si-Si bond is shorter than that of Si with a diamond structure. This is attributed to a higher carrier mobility and lower thermoelectric performance. The other parts in the crystal lattice of $TiMnSi_2$, except for the Si-Si bond, consist of

Ti-Mn-Si ternary bent bonds. The Ti-Mn-Si ternary blocks contribute to the electronic performance; however, it is thought that they do not strongly influence the electronic properties.

In this study, the lattice thermal conductivity of the studied compounds is expected to be as low as that of skutterudite compounds, which contain large open spaces and exhibit low thermal conductivity[15,16]. However, a high resistance to heat transfer in the lattice, such as that observed in a skutterudite structure, was not realized. This is because the bond was more metallic than expected, and a relatively high thermal conductivity of $Zr_3Mn_4Si_6$ shows fast thermal diffusion due to the free transfer of electronic carriers along the strong Si-Si bond. To verify this hypothesis, the measurement of the Hall coefficient and the analysis of $D(E)$ at E_F will be performed in future studies.

The thermoelectric performance can be further enhanced by reducing the number of carrier electrons by elemental replacement. The Si-Si bond should be lengthened, for example, by expanding the blocks of $Ti_2Mn_3Si_4$ or by inserting foreign elements in the Si-Si layer. A more detailed study is required in order to verify whether the characteristic structures of these compounds can be maintained even when the elements are replaced.

Conclusions

Because $Zr_3Mn_4Si_6$ and $TiMnSi_2$ possess a complex crystalline structure and open spaces in the lattice, low thermal conductivity was expected. The thermal conductivity was as low as that of other intermetallic compounds, but higher than that of skutterudite. The dimensionless figures of merit ZT were 1.92×10^{-3} and

2.76×10^{-3} for $Zr_3Mn_4Si_6$ and $TiMnSi_2$, respectively. One of the reasons why the Seebeck coefficient and the electric resistivity were low may be the strong Si-Si bond in their crystal structure. The Si-Si bond length is shorter than that of silicon with a diamond structure, and heat as well as electronic carriers can be easily transferred. The thermoelectric performance can be further enhanced by arranging the layer having a short Si-Si bond and by controlling the number of carrier electrons by elemental replacement.

Acknowledgment

The authors would like to express their sincere gratitude to Mr. Kenji Ohkubo, Hokkaido University, for his kind technical assistance during the measurement of thermal conductivity by laser-flash method. This work is financially supported in part by The Core Research of Evolutional Science & Technology (CREST) program of the Japan Science and Technology Agency (JST).

References

1. R. O. Suzuki and D. Tanaka: J. Power Sources, **122** [2] (2003) 201-209.

2. R. O. Suzuki and D. Tanaka: J. Power Sources, **124** [1] (2003) 293-298.

3. R. O. Suzuki and D. Tanaka: J. Power Sources, **132** [1-2] (2004) 266-274.

4. R. O. Suzuki: J. Power Sources, **133** [2] (2004) 277-285.

5. I. Matsubara, Y. Zhou, T. Takeuchi, R. Funahashi, M. Shikano, N. Murayama, W. Shin and N. Izu: J. Ceram. Soc. Jpn., **111** [4] (2003) 238-241.

6. L. Siwen, R. Funahashi, I. Matsubara, H. Yamada, K. Ueno and S. Sodeoka: Ceram. Intern., **27** [3] (2001) 321-324.

7. Y. Miyazaki, K. Kudo, M. Akoshima, Y. Ono, Y. Koike and T. Kajitani: J. Appl. Phys., **39** (2000) 531–533.

8. I. Terasaki, Y. Sasago and K. Uchinokura: Phys. Rev. B **56** [20] (1997) 685-687.

9. Y. Hanada, R. O. Suzuki and K. Ono: J. Alloy. Compd., **329** [1-2] (2001) 63-68.

10. Y. Nishino: Intermetallics, **8** (2000) 1233-1241.

11. A. V. Tkachuk, S. J. Crerar and A. Mar: J. Solid State Chem., **177** (2004) 3939-3943.

12. J. Steinmentz, G. Venturini and B. Roques: Acta Crystallogr., Sec. B, **38**, (1982) 2103-2108.

13. N. F. Mott and H. Jones: *The theory of the properties of metals and alloys*, (Oxford University Press, London, 1943).

14. N. A. Lange and J. A. Dean: *Lange's Handbook of Chemistry*, (McGraw-Hill, New York, 1979) p.3-2–3-6.

15. G. S. Nolas, G. Fowler and J. Yang: J. Appl. Phy., **100** [4] (2006) 43705-1-4.

16. B. C. Sales, D. Mandrus and R. K. Williams: Science, **272** (1996) 1325-1328.

Table Captions

Table 1 Compositional analysis of $Zr_3Mn_4Si_6$.

Table 2 Specific heat and thermal conductivity at room temperature.

Figure Captions

Fig. 1 Crystal arrangements of $Zr_3Mn_4Si_6$ and $TiMnSi_2$.

Fig. 2 Temperature dependency of Seebeck coefficient.

Fig. 3 Temperature dependency of electrical resistivity.

Fig. 4 Temperature dependency of thermal diffusivity.

Fig. 5 Temperature dependency of heat capacity.

Fig. 6 Temperature dependency of thermal conductivity.

Fig. 7 Dimensionless figure of merit *ZT*.

Fig. 8 Crystal structure of $Zr_3Mn_4Si_6$. (a)-(c) show a magnified view of the connections in a part of the crystal shown in (d). Mn, Zr, and Si atoms are represented by large black spheres, large white spheres, and small spheres, respectively.

Fig. 9 Magnified view of the connections in a part of crystal structure of $TiMnSi_2$, where the Mn, Ti, and Si atoms are represented by the large black spheres, large white spheres, and small spheres, respectively.

Table 1 Compositional analysis of $Zr_3Mn_4Si_6$.

Element	Composition (mol%)	
	Stoichiometric	Measured
Si	46.1	49.1
Mn	30.8	29.3
Zr	23.1	21.6

Table 2 Specific heat and thermal conductivity at room temperature.

	Specific heat, C_p/Jmol^{-1}K^{-1}		Thermal conductivity, κ/Wm^{-1}K^{-1}	
	Estimated	Measured	Estimated	Measured
$TiMnSi_2$	0.60	0.568	5.31	6.63
$Zr_3Mn_4Si_6$	0.53	0.433	10.19	8.26

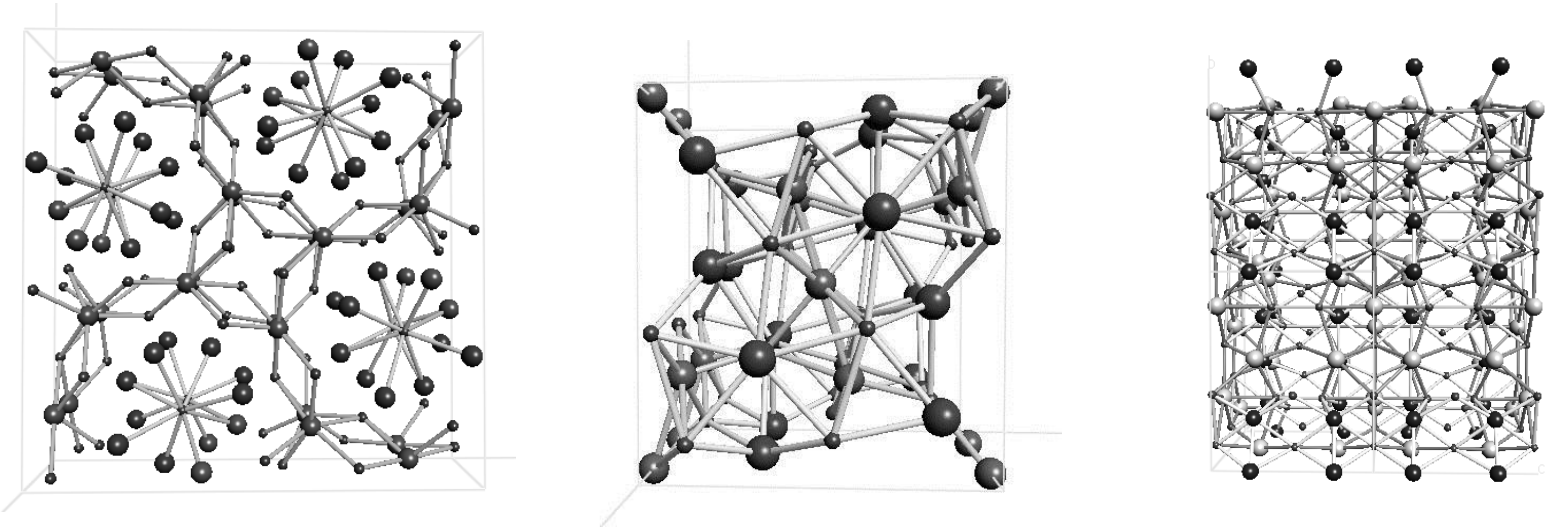

(a) $Zr_3Mn_4Si_6$ (b) $TiMnSi_2$ (c) $TiMnSi_2$

Fig.1 Crystal arrangements of $Zr_3Mn_4Si_6$ and $TiMnSi_2$.

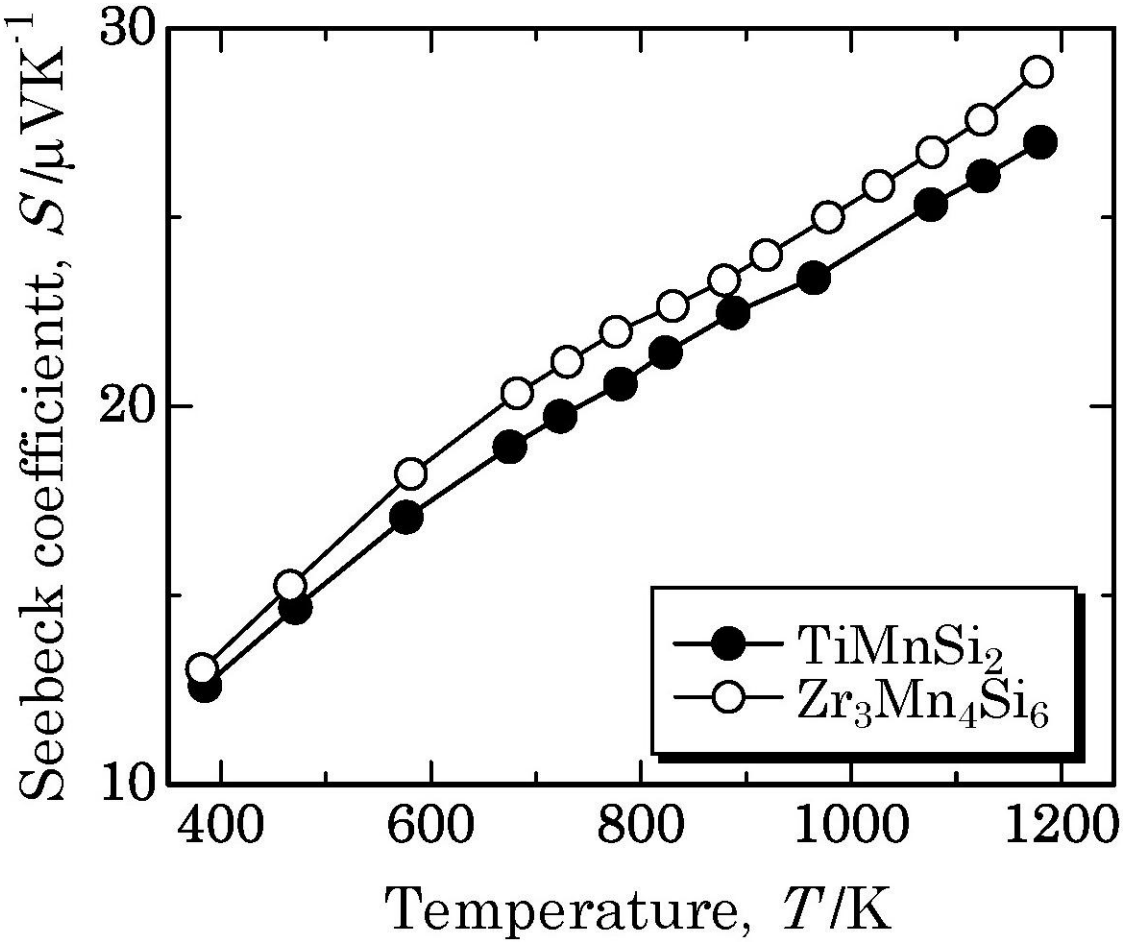

Fig.2 Temperature dependency of Seebeck coefficient.

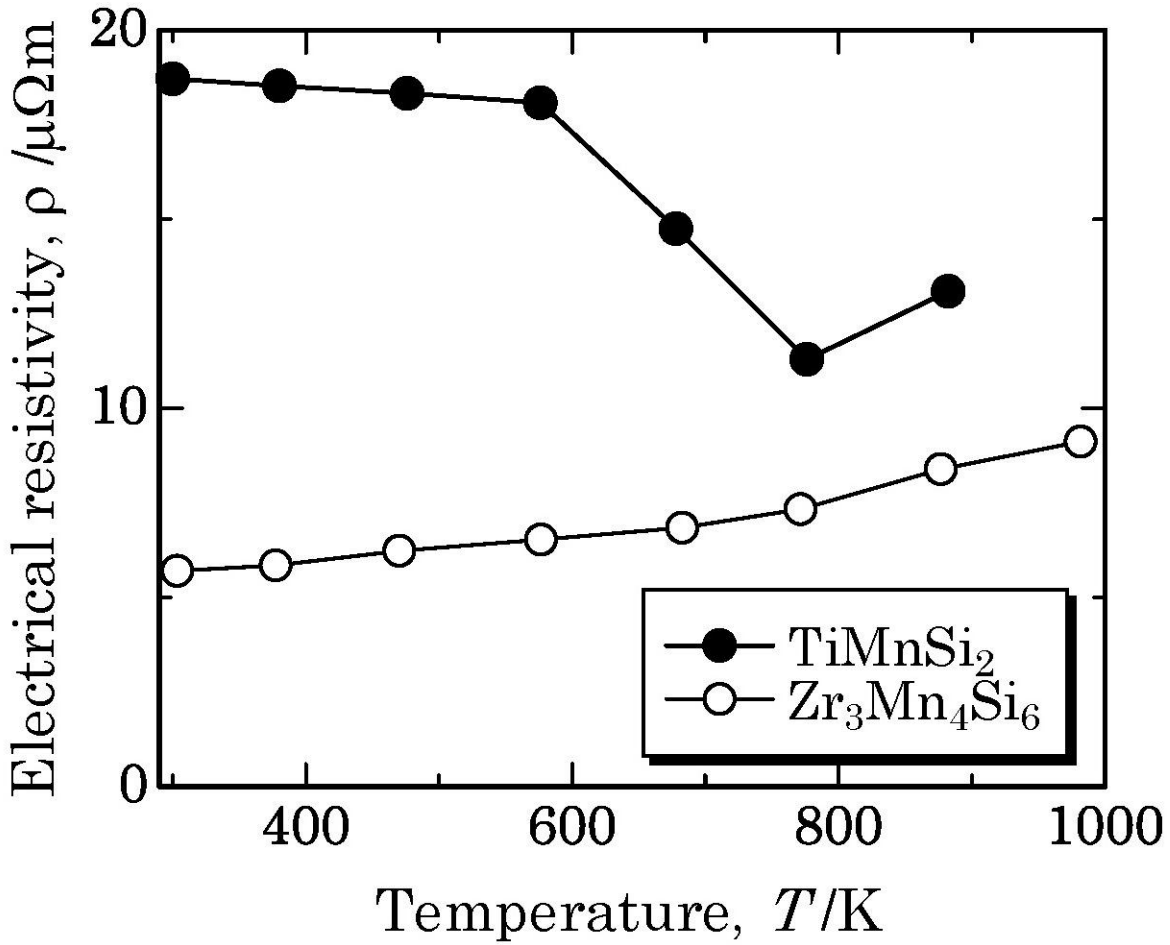

Fig.3 Temperature dependency of electrical resistivity.

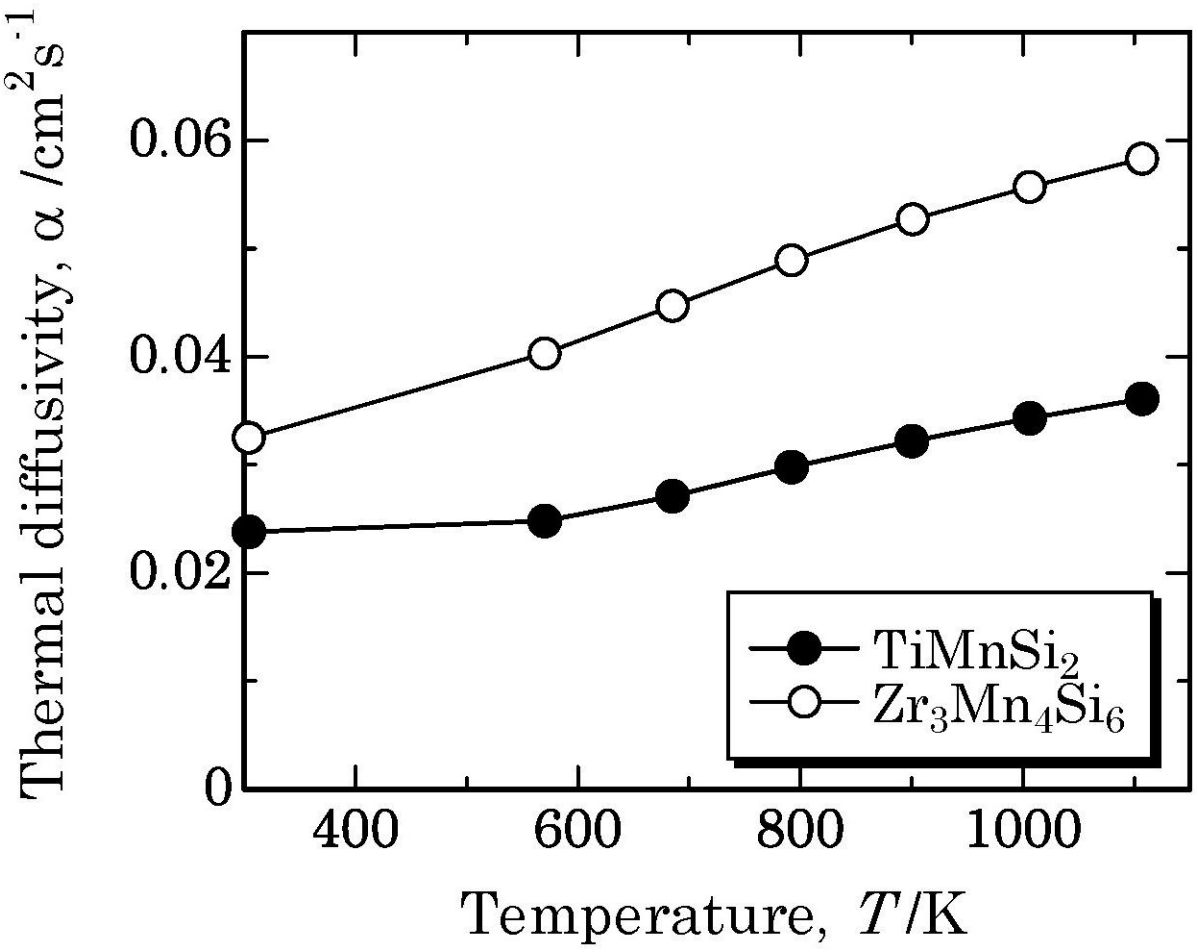

Fig.4 Temperature dependency of thermal diffusivity.

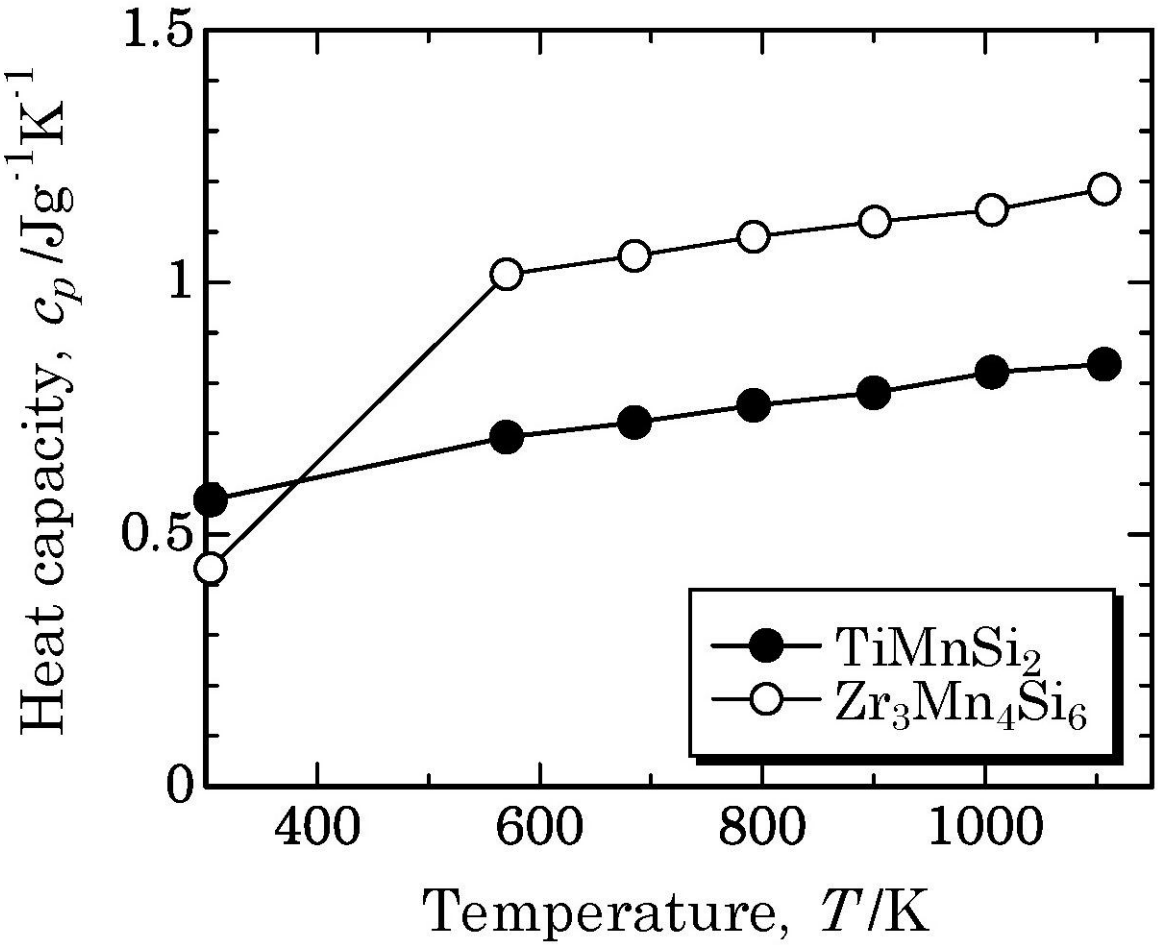

Fig.5 Temperature dependency of heat capacity.

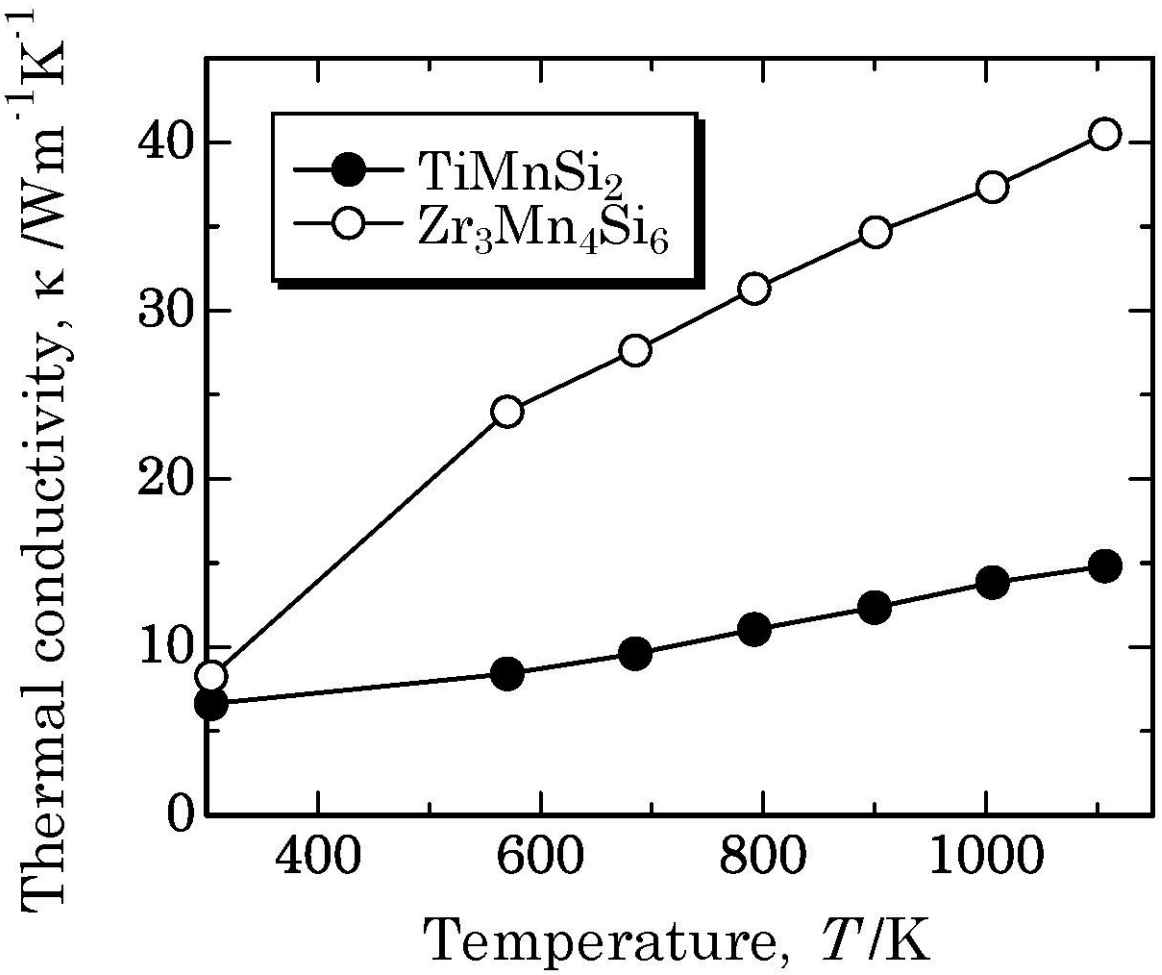

Fig.6 Temperature dependency of thermal conductivity.

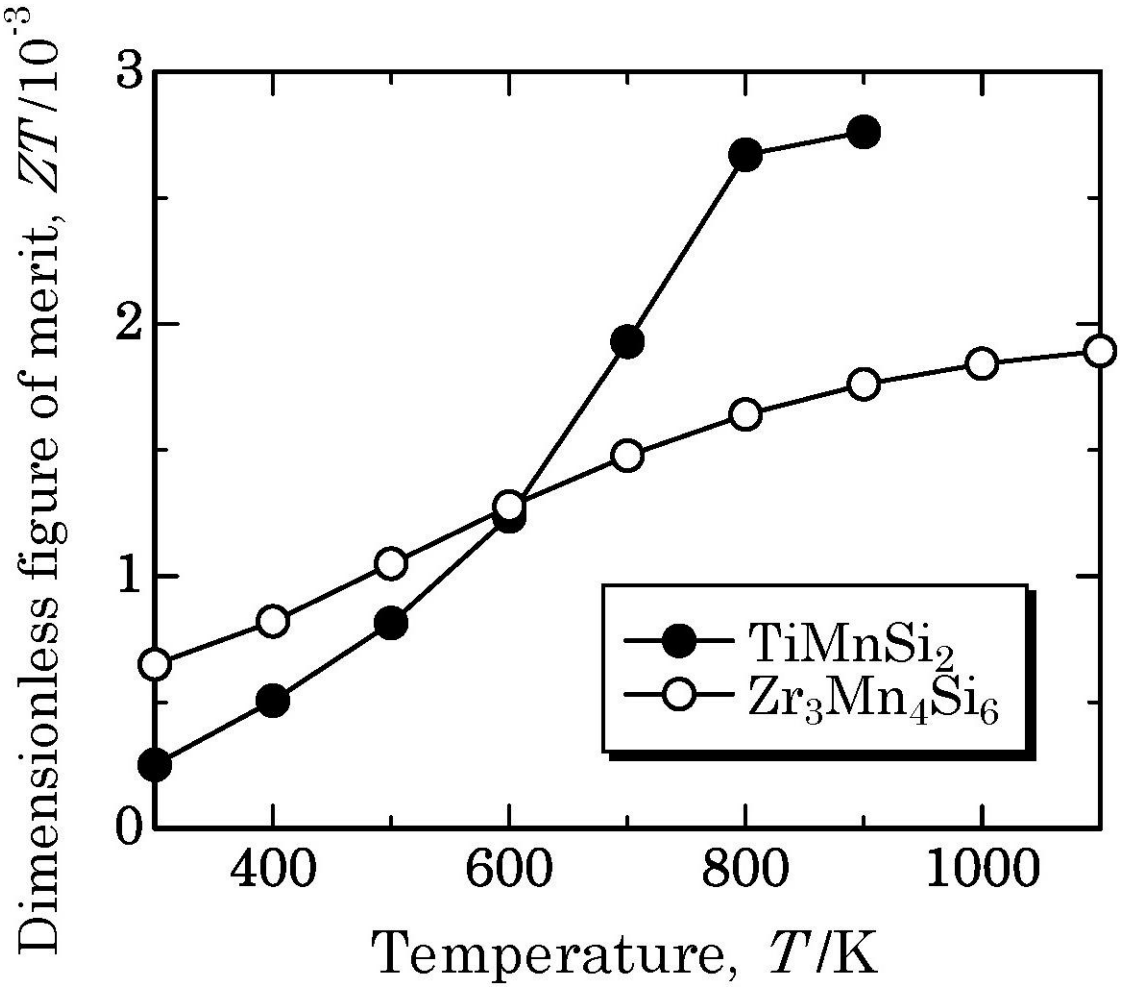

Fig.7 Dimensionless figure of merit *ZT*.

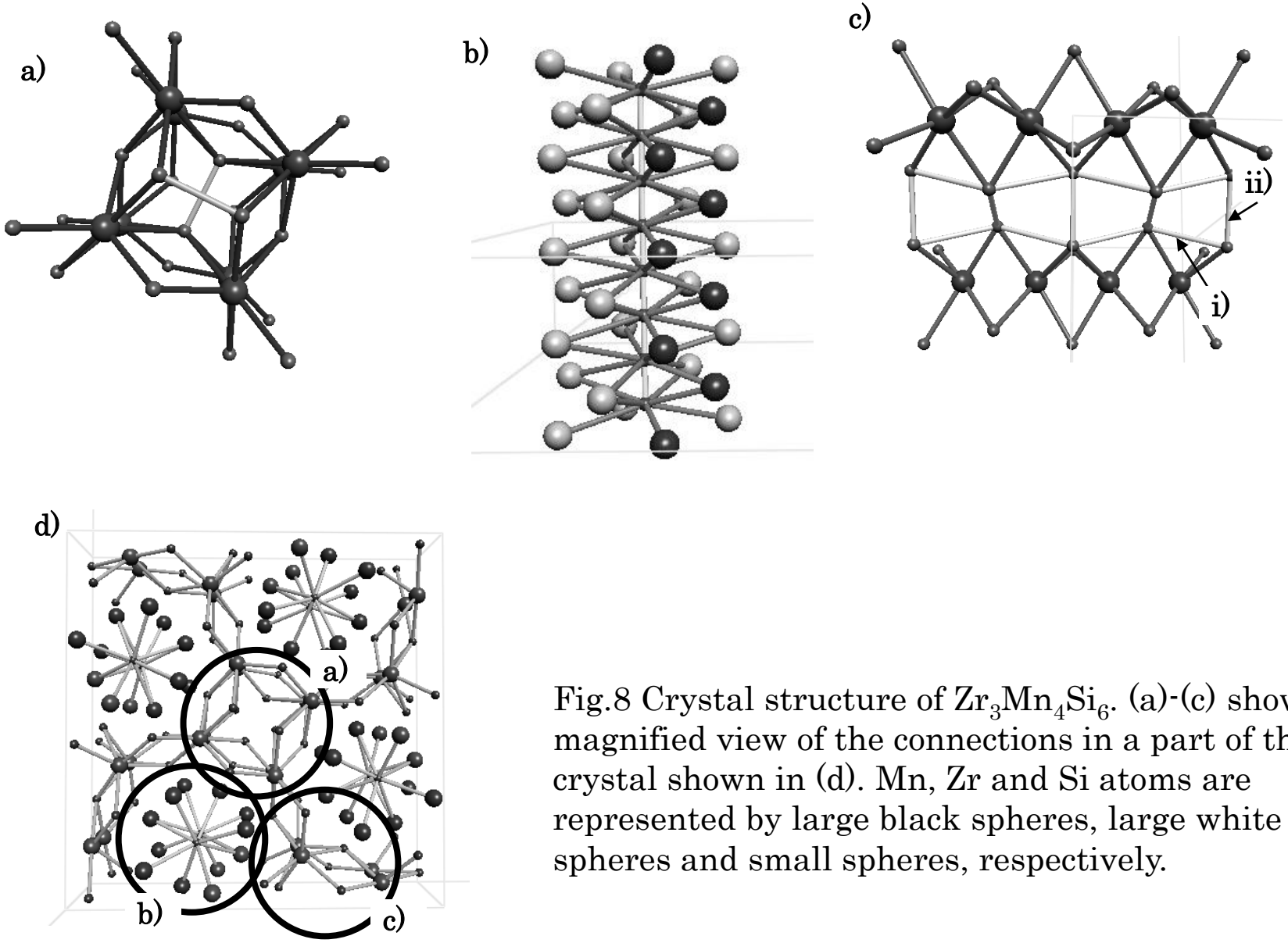

Fig.8 Crystal structure of $Zr_3Mn_4Si_6$. (a)-(c) show a magnified view of the connections in a part of the crystal shown in (d). Mn, Zr and Si atoms are represented by large black spheres, large white spheres and small spheres, respectively.

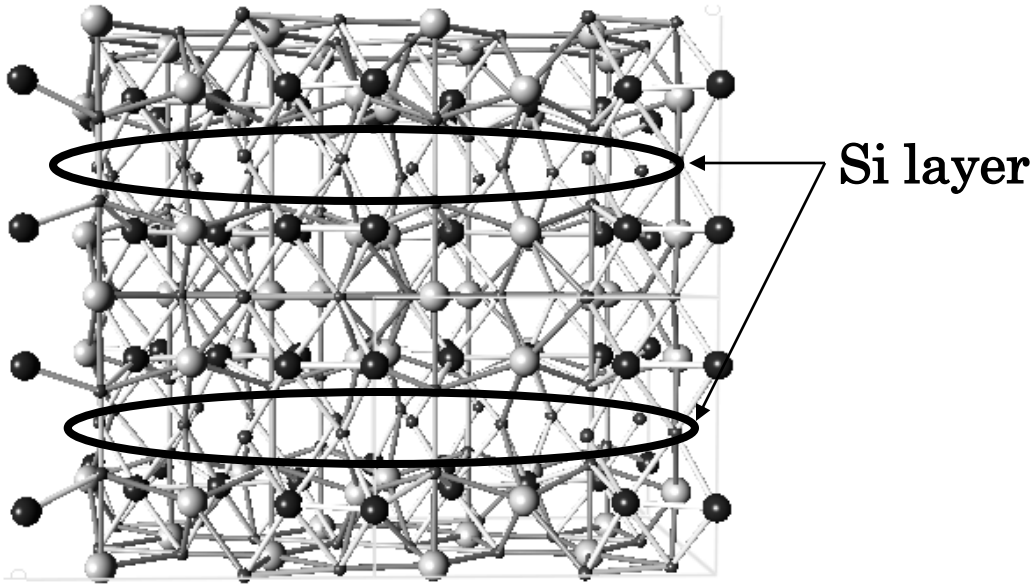

Fig.9 Magnified view of the connections in a part of crystal structure of $TiMnSi_2$, where the Mn, Ti and Si atoms are represented by the large black spheres, large white spheres, and small spheres, respectively.